PHYSICAL REVIEW B VOLUME 15, NUMBER 10 15 MAY 1977

# $LMM$ Auger spectra of Cu, Zn, Ga, and Ge. II. Relationship with the $L_{23}$ photoelectron spectra via the $L_2L_3M_{45}$ Coster-Kronig process

E. Antonides, E. C. Janse, and G. A. Sawatzky
*Laboratory of Physical Chemistry, Materials Science Center, University of Groningen, The Netherlands*
(Received 17 December 1976)

In this paper we present conclusive experimental evidence that the Auger satellite structure on the low-kinetic-energy side of the $L_3M_{45}M_{45}$ Auger spectra in Cu and Zn is a direct result of the $L_2L_3M_{45}$ Coster-Kronig transition preceding the Auger transition. The position of the satellite structure is compared with numerical calculations of the final state for the ionized atoms. The same Coster-Kronig process is shown to be responsible for the anomalous intensity ratio of the $L_2M_{45}M_{45}$ to $L_3M_{45}M_{45}$ Auger spectra. From this intensity ratio the Auger part of the $L_{23}$ photoelectron linewidths can be determined and is shown to be in reasonable agreement with theoretical values.

## I. INTRODUCTION

In a recent paper,[1] hereafter referred to as I, we discussed the $LMM$ Auger spectra of Cu, Zn, Ga, and Ge, and we showed that with detailed transition-probability calculations a clear assignment can be made of the observed structure to the various final-state terms. We also showed that the "on-site" Coulomb interaction can be obtained from a combination of the Auger and x-ray photoelectron spectra and that detailed information concerning the various Slater integrals can be obtained from the experimental term splittings.

In this paper we will discuss the often anomalous intensity ratios of the $L_2$ and $L_3$ parts of the $L_{23}MM$ Auger spectra as well as the Auger vacancy satellite structure in the $L_3M_{45}M_{45}$ region. We will show that these anomalies are a result of a Coster-Kronig process which precedes the Auger process. We also show that the intensity ratio of the $L_2M_{45}M_{45}$ to $L_3M_{45}M_{45}$ Auger spectra can be used to predict the Auger part of the $L_2$ and $L_3$ photoelectron linewidths. These predictions are compared with theoretical values.

The influence of the above-mentioned Coster-Kronig process on the intensity ratios of the $L_2M_{45}M_{45}$ and $L_3M_{45}M_{45}$ Auger spectra, on the Auger vacancy structure in the $L_3M_{45}M_{45}$ spectrum and on the $L_{23}$ photoelectron spectrum have been discussed in recent publications.[2-6] However, this has been done in a very qualitative way. The major aim of this paper is to give a simple and quantitative description of the relationship between the $L_2L_3M_{45}$ Coster-Kronig process and both the Auger and x-ray photoelectron spectra. Since the Coster-Kronig effects are most evident in the $L_{23}M_{45}M_{45}$ region, we will limit our discussion to this portion of the Auger spectrum.

## II. EXPERIMENTAL

The x-ray Auger spectra and the x-ray photoelectron spectra were collected with an AEI-ES200 spectrometer using a Mg $K\alpha$ source for the Auger spectra, except for Ge, in which case monochromatized Al $K\alpha$ radiation was used to avoid threshold effects in the $L_2$ level (see I). The $L_{23}$ photoelectron spectra were obtained with monochromatized Al $K\alpha$ radiation. The linewidth of this source as determined from the Ag Fermi cutoff was about 0.5 eV. Further experimental details are given in I. All spectra were corrected for the energy-dependent transmission of the analyzer and for secondary scattered electrons. A detailed description of these corrections is also given in I.

## III. RESULTS AND DISCUSSION

In Fig. 1 the $L_{23}M_{45}M_{45}$ Auger spectra of Cu, Zn, Ga, and Ge are shown on a relative energy scale. Aside from the overall resemblance between the spectra of the four materials there are also certain differences. The most important features to be noticed are the following:

(a) The relative intensity of the $L_2$ part of the spectra as compared with the $L_3$ part is increasing in going from Cu to Ga, staying approximately constant in going from Ga to Ge.

(b) In Cu and Zn there exists extra structure on the low-energy side of the $L_3M_{45}M_{45}$ Auger spectrum which is not present in Ga and Ge. Both features (a) and (b) can be explained by the occurrence of the $L_2L_3M_{45}$ Coster-Kronig process. This process is schematically represented in Fig. 2. A primarily created $L_2$ hole converts to an $L_3$ hole thereby ejecting an $M_{45}$ electron. The necessary condition for the process to appear is that the $L_3 - L_2$ energy difference due to spin-orbit coupling, must exceed the binding energy of the $M_{45}$ electron, in the presence of the $L_2$ hole. This condition is easily satisfied for Cu and to a lesser extent for Zn, but not for Ga and Ge.[2,4]

When the $L_2L_3M_{45}$ Coster-Kronig process occurs, a fraction of the primarily created $L_2$ holes decays via this extra path, thereby reducing the probabil-

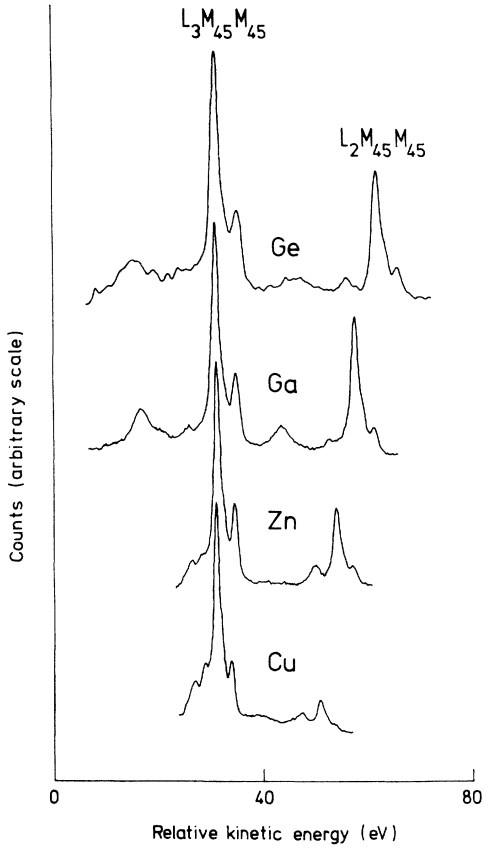


FIG. 1. $L_{23}M_{45}M_{45}$ Auger spectra of Cu, Zn Ga, and Ge. The kinetic energy for the different metals has been shifted such that the most intense lines come at the same position.

ity that they decay via the $L_2MM$ Auger processes. This Coster-Kronig process therefore reduces the intensity of the $L_2$ part of the latter processes as compared to the $L_3$ part explaining qualitatively the above mentioned feature (a).

After the $L_2L_3M_{45}$ Coster-Kronig process has taken place the $L_3$ hole can decay via the normal $L_3MM$ Auger processes, except that the initial state already has a hole in the $M_{45}$ level. For the $L_3M_{45}M_{45}$ case this is represented in Fig. 3. The process will now end up in a final state with *three* $M_{45}$ holes. The difference between this Coster-Kronig preceded $L_3M_{45}M_{45}$ process and the common $L_3M_{45}M_{45}$ process gives rise to a shift to lower kinetic energy of the former one, because of the Coulomb interaction between the Auger electrons and the extra $M_{45}$ hole, and this is a qualitative explanation for feature (b).[5,6]

Recently, Roberts *et al.*[3] estimated this Auger vacancy shift for Cu to be of the same order as the chemical shifts reported on the $L_3M_{45}M_{45}$ Auger lines in various copper compounds, namely 1–2

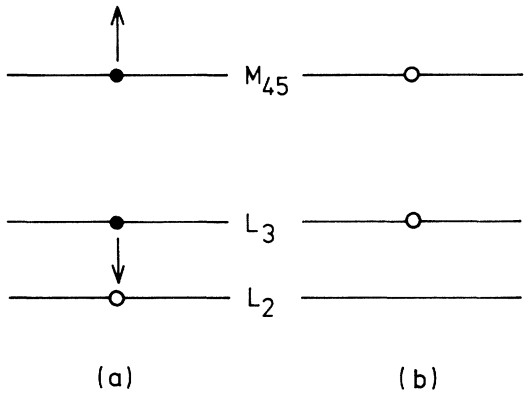


FIG. 2. Schematic representation of the $L_2L_3M_{45}$ Coster-Kronig process: (a) initial state; (b) final state.

eV. This is a rather bad approximation because it is known that the extra-atomic relaxation energies are strongly dependent on the electronic structure of the material. This value is much less than the experimental Auger vacancy shift, for which they found a value of about 7 eV. We therefore estimated this shift ($\Delta E$) from calculated total energies of the initial, intermediate, and final state ions in terms of which $\Delta E$ will be given by

$$\Delta E = [E(2p^1) - E(3d^2)] - [E(2p^1 3d^1) - E(3d^3)]. \quad (1)$$

Here $E(X)$ stands for the total energy of the ion with a hole configuration $X$. The first quantity between brackets in Eq. (1) can be written

$$E(2p^1) - E(3d^2) = E_b(2p) - 2E_b(3d) - \mathfrak{F}(3d^2) + R_{at}(3d^2) + R_{ea}(3d^2) - \delta(E). \quad (2)$$

This result can be obtained by using Eq. (1) in I. $E_b(2p)$ and $E_b(3d)$ are free-atom binding energies, which are distinguished from the binding energies

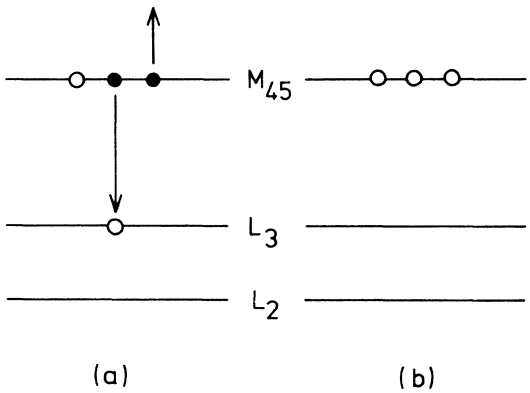


FIG. 3. Schematic representation of the $L_3M_{45}M_{45}$ Auger process after the $L_2L_3M_{45}$ Coster-Kronig process has taken place (see Fig. 2): (a) initial state; (b) final state.

TABLE I. Values for the atomic part of the Auger vacancy shift $\Delta E_{at}$, extra-atomic relaxation energy $R_{ea}$, and calculated and experimental Auger vacancy shift $\Delta E$ (eV). See text.

| | $\Delta E_{at}$ | $R_{ea}(3d^2)$ | $\Delta E$ Calc. | $\Delta E$ Expt. |
|---|---|---|---|---|
| Cu | 19.2 | 12.9 | 6.3 | 5.0 |
| Zn | 21.4 | 14.6 | 6.8 | 6.5 |

in the metal by an additional extra-atomic energy $\delta E$. $\mathfrak{F}(3d^2)$ describes the Coulomb energy of two $3d$ holes, $R_{at}(3d^2)$ and $R_{ea}(3d^2)$ are the atomic and extra-atomic parts, respectively, of the total relaxation energies defined in I. We will assume that the extra-atomic relaxation energies are independent of the electronic configurations of the ion. That is we will assume it to be the same for the $2p$ as for a $3d$ hole. This is a reasonable approximation because the extra-atomic relaxation energies will be determined by more long-range Coulomb interactions and will depend mainly on the charge of the ion and not strongly on its electronic configuration. For the second quantity between brackets in Eq. (1) we can follow the same argument and the final result can be written

$$\Delta E = \Delta E_{at} + R_{ea}(2p^1 3d^1) + R_{ea}(3d^2) - R_{ea}(3d^3) . \quad (3)$$

Here again as just mentioned we will take $R_{ea}(2p^1 3d^1) = R_{ea}(3d^2)$. $\Delta E_{at}$ is the atomic part of the Auger vacancy shift $\Delta E$ which can be determined from the total energies of the states appearing in Eq. (1). These total energies are obtained from numerical Hartree-Fock calculations on the corresponding final-state atom, averaged over their final-state terms.

The extra-atomic relaxation energies $R_{ea}(3d^2)$ and $R_{ea}(3d^3)$ are the relaxation energies which cause a reduction in the effective Coulomb energy of two or three $3d$ holes, respectively. These reductions are due to the interaction of a hole with the polarization cloud produced by the *other* holes present. The interaction of a hole with its own polarization cloud is already taken into account in the one hole energies. For linear response we can write

$$R_{ea}(3d^2) = 2 \times \text{the one-hole extra-atomic relaxation energy} \quad (4a)$$

and

$$R_{ea}(3d^3) = 6 \times \text{the one-hole extra-atomic relaxation energy} . \quad (4b)$$

We can then write from Eq. (3)

$$\Delta E = \Delta E_{at} - R_{ea}(3d^2) . \quad (5)$$

Values for $R_{ea}(3d^2)$ now can be deduced from the results of Table VI in I by subtracting the atomic relaxation energy from the total relaxation energy. The results are summarized in Table I. The experimental values for $\Delta E$ were obtained assuming that the two most prominent peaks in the Auger vacancy satellite structure of the $L_3M_{45}M_{45}$ spectrum (indicated as $a_1$ and $b_1$ in Fig. 4) correspond to the most prominent lines of the $L_3M_{45}M_{45}$ Auger spectrum itself (indicated as $a_2$ and $b_2$ in Fig. 4.) From Table I we now can see that the calculated and experimental values for $\Delta E$ are in very good agreement.

In the foregoing discussion we have assumed the lifetime of the $3d$ hole to be longer than the lifetime of the $L_3$ hole. At first glance this may not seem to be the case because of the relatively large one-electron $3d$ bandwidth. In the Coster-Kronig process however the $3d$ and $L_3$ hole are, initially at least, on the same atom and therefore the $3d$ hole will not behave as a single-particle excitation and the width or lifetime of such a state cannot be compared to the one-particle bandwidth. That the lifetime of such a state is much larger than that derived from the one-electron bandwidth is also evident from the narrow, atomiclike Auger spectra in these metals. In the latter case the final state is also two holes on one atom and apparently has a very long lifetime. The fact that the satellites due to the Coster-Kronig process are present and reasonably narrow in the $L_3M_{45}M_{45}$ Auger spec-

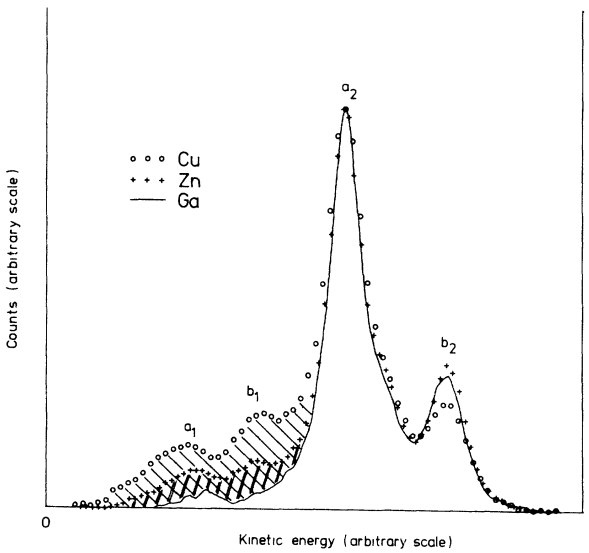


FIG. 4. Comparison of the shape of the $L_3M_{45}M_{45}$ Auger spectrum of Cu and Zn to that of Ga. The energy scale is different for the three metals in order to make the splitting between the two most prominent lines in the spectra (indicated as $a_2$ and $b_2$) the same. The two differently shaded areas indicate the Auger vacancy satellite structure of Cu and Zn.

TABLE II. Values for the $L_3M_{45}M_{45}$ to $L_2M_{45}M_{45}$ intensity ratio including the Auger vacancy satellite structure and corrected for this structure, respectively. The intensity of the Auger vacancy structure relative to the total intensity of the $L_3M_{45}M_{45}$ Auger spectrum is also given.

| | $I(L_3M_{45}M_{45})/I(L_2M_{45}M_{45})$ With satellite structure | Without satellite structure | Intensity satellite structure (%) |
|---|---|---|---|
| Cu | 7.6 | 1.6 | 30±2 |
| Zn | 3.0 | 1.9 | 13±3 |
| Ga | ... | 1.6 | ... |
| Ge | ... | 1.9 | ... |

trum is direct evidence that the intermediate state with an $L_3$ and $3d$ hole must be long lived as compared to the Auger lifetime of the $L_3$ hole. If the lifetime of the intermediate state were short, the Coster-Kronig preceded $L_3M_{45}M_{45}$ Auger spectra would be indistinguishable in position from the ordinary Auger spectra.

We now will show that features (a) and (b) are quantitatively related to each other. First of all we want to know what fraction of the intensity of the $L_3M_{45}M_{45}$ spectrum of Cu and Zn is caused by the $L_2L_3M_{45}$ Coster-Kronig process. To do this we compared the shape of the Cu and Zn spectra to that of Ga in which the satellite structure does not appear. In this way a fairly accurate estimate can be made of the intensity of the extra satellite structure in the Cu and Zn spectra. The result of this comparison is shown in Fig. 4. The two differently shaded areas in this figure correspond to the Auger vacancy satellite structure for Cu and Zn. At this point we have to keep in mind that these intensities are so to speak stolen from the $L_2M_{45}M_{45}$ Auger spectrum, because by the $L_2L_3M_{45}$ Coster-Kronig process $L_2$ holes are transferred to the $L_3$ level (see Fig. 3). Therefore, if we would subtract these extra intensities from the $L_3M_{45}M_{45}$ Auger spectrum and add it to the $L_2M_{45}M_{45}$ spectrum, we then would expect that the in this way corrected $L_3M_{45}M_{45}$ and $L_2M_{45}M_{45}$ spectra would give an intensity ratio of about the same value as in Ga and Ge where the Coster-Kronig process is not present. These corrected intensity ratios are given in Table II. The intensities used to calculate the ratios shown in this table were obtained by integrating the spectrum after the analyzer and scattering correction mentioned above had been carried out. We clearly see from this table that if the intensity ratios of Cu and Zn are corrected for the intensity of the Auger vacancy satellite structure in the way just discussed, then their values are close to those of Ga and Ge, and also close to the value of 2 which would be expected from the multiplicities of the $L_2$ and $L_3$ level. This conclusively shows that the satellite structure and the anomalous intensity ratio of the $L_2M_{45}M_{45}$ to $L_3M_{45}M_{45}$ Auger spectra are directly related to and result from the $L_2L_3M_{45}$ Coster-Kronig process.

We now turn to the $L_{23}$ photoelectron spectrum of Cu, Zn, Ga, and Ge, which are shown in Fig. 5. From these spectra the following can clearly be seen. In going from Cu to Ga the widths of the $L_2$ line as compared to the $L_3$ line is decreasing. This phenomenon, like features (a) and (b) mentioned before, can be related to the $L_2L_3M_{45}$ Coster-Kronig process. The occurrence of this process leads to a lifetime broadening of the $L_2$ level as compared to the $L_3$ level, because it exclusively shortens the lifetime of the $L_2$ hole. The values of the widths and the intensity ratios $I_{L_3}/I_{L_2}$ are listed in Table III. From this table it can be seen that $\Gamma_{L_2}$ decreases monotonically on going from Cu to Ga and then increases for Ge. This

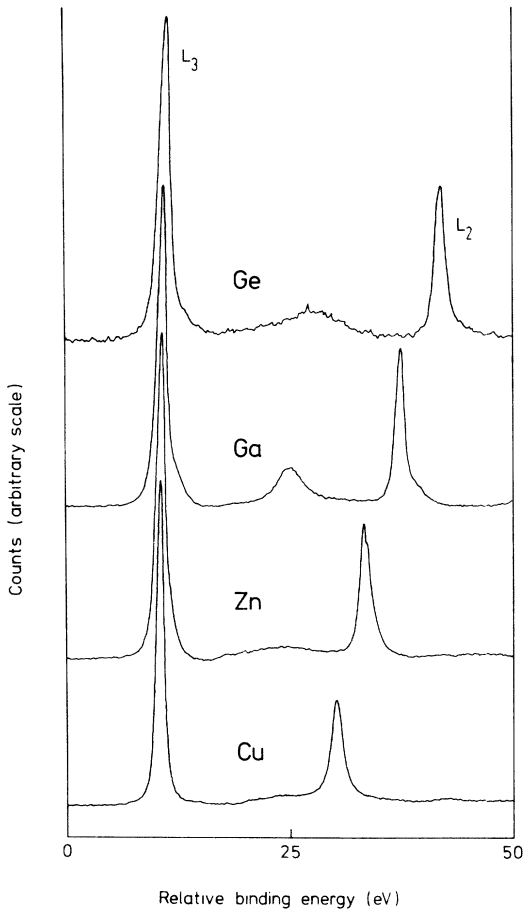


FIG. 5. $L_{23}$ photoelectron spectra of Cu, Zn, Ga, and Ge. The energy scale has been shifted such that the $L_3$ lines come at the same position.

TABLE III. Values for the total linewidths $\Gamma_{L_2}$ and $\Gamma_{L_3}$ of the $L_2$ and $L_3$ level, respectively (eV), and for the $L_3$ to $L_2$ intensity ratio.

| | $I(L_3)/I(L_2)$ | $\Gamma_{L_2}$ | $\Gamma_{L_3}$ |
|---|---|---|---|
| Cu | 2.0 | 1.54 ± 0.05 | 0.98 ± 0.05 |
| Zn | 2.0 | 1.48 ± 0.05 | 1.18 ± 0.05 |
| Ga | 1.9 | 1.16 ± 0.05 | 1.17 ± 0.05 |
| Ge | 1.9 | 1.44 ± 0.05 | 1.42 ± 0.05 |

may be due to the fact that Ge is a semiconductor in which band bending at the surface and/or nonuniform charging are important contributions to the bandwidth. The values are obtained from a least-squares fit to the $L_{23}$ photoelectron spectra. The line shape of the fit was taken to be the sum of Lorentzian and Gaussian character, while the ratio of the Lorentzian to Gaussian character was constrained to be equal for both the $L_2$ and $L_3$ line. From Table III we see that the intensity ratio $I_{L_3}/I_{L_2}$ is about 2 for all four metals, indicating that the number of initially created $L_3$ holes is about two times that of the $L_2$ holes, as is expected from the multiplicity ratio of the $L_2$ and $L_3$ level.

We now come to a quantitative comparison of the $L_{23}M_{45}M_{45}$ Auger spectrum with the $L_{23}$ photoelectron spectrum, both of which are, as we have seen, influenced by the $L_2L_3M_{45}$ Coster-Kronig process. Since the intensity of the most prominent line in the $L_3M_{45}M_{45}$ Auger spectrum, corresponding to the $^1G$ final-state term,[1] will only be very weakly affected by the Auger vacancy satellite structure we can use the intensity of this line for an accurate determination of the $L_3M_{45}M_{45}$ to $L_2M_{45}M_{45}$ intensity ratio. For this intensity ratio we can write

$$I_{1_G}(L_3M_{45}M_{45})/I_{1_G}(L_2M_{45}M_{45}) = 2(\Gamma_A + \Gamma_{CK})/\Gamma_A . \quad (6)$$

Here $\Gamma_A$ is the Auger part of the total $L_2$ and $L_3$ width. We assume $\Gamma_A$ to be approximately the same for both levels.[2] $\Gamma_{CK}$ is the difference between $\Gamma_{L_2}$ and $\Gamma_{L_3}$, the total linewidth of the $L_2$ and $L_3$ level, respectively. As discussed before this difference can completely be ascribed to the $L_2L_3M_{45}$ Coster-Kronig process. The factor 2 arising in the right-hand side of Eq. (6) is introduced to account for the multiplicity ratio of the $L_2$ and $L_3$ level. From Eq. (6) we see that when the Coster-Kronig process is absent the intensity ratio will take the theoretical value of 2. The value of $\Gamma_A$ is difficult to obtain explicitly because aside from $\Gamma_A$, the measured total width $\Gamma_{L_3}$ of the $L_3$ level will be determined by the instrumental broadening, the natural linewidth of the source, electron-phonon interactions, many-electron effects, etc. (the effect of fluorescence processes on the total linewidth can be neglected[2]). Therefore we calculated $\Gamma_A$ for Cu and Zn from the experimental values for $I_{1_G}(L_3M_{45}M_{45})/I_{1_G}(L_2M_{45}M_{45})$ and $\Gamma_{CK}$, using Eq. (6). The values of $I_{1_G}(L_3M_{45}M_{45})/I_{1_G}(L_2M_{45}M_{45})$, $\Gamma_{CK}$, and of the resulting $\Gamma_A$ are listed in Table IV. Another way to obtain a value for $\Gamma_A$ is to sum up the transition rates of all Auger transitions starting with a hole in the $L_2$ or $L_3$ level, which have been calculated by McGuire.[7] $\Gamma_A$ now is the result of this addition divided by 2.[8] The values for $\Gamma_A$ obtained in this way are also listed in Table IV (Cu, Ga, and Ge were interpolated). Finally Yin *et al.*[2] have calculated $\Gamma_A$ for Cu and Zn. Their values are given in the same table. From this table we can see that the values for $\Gamma_A$ obtained from Eq. (6) are reasonably close to the other values.

## IV. CONCLUSIONS

In conclusion we have shown that there exists a close relationship between the $L_{23}M_{45}M_{45}$ Auger spectrum and the $L_{23}$ photoelectron spectrum, which is caused by the $L_2L_3M_{45}$ Coster-Kronig process and which can be described in a quantitative way. The shift of the Auger vacancy structure is calculated and shown to be in good agreement with the experimental value.

TABLE IV. Coster-Kronig widths $\Gamma_{CK}$ (equal to the $L_2, L_3$ linewidth difference, see Table III) in eV, Auger widths $\Gamma_A$ in eV, and intensity ratios of the $^1G$ line in the $L_3M_{45}M_{45}$ spectrum to that in the $L_2M_{45}M_{45}$ spectrum. The latter ratios have been obtained from a least-squares fit to the spectra: (a) using Eq. (6); (b) from McGuire (Ref. 7) averaged over the $L_2$ and $L_3$ level; (c) from Yin *et al.* (Ref. 2) averaged over the $L_2$ and $L_3$ level.

| | $\Gamma_{CK}$ | $I_{1_G}(L_3M_{45}M_{45})/I_{1_G}(L_2M_{45}M_{45})$ | $\Gamma_A$ (a) | $\Gamma_A$ (b) | $\Gamma_A$ (c) |
|---|---|---|---|---|---|
| Cu | 0.56 | 5.3 ± 0.3 | 0.34 ± 0.05 | 0.36 | 0.53 |
| Zn | 0.30 | 2.8 ± 0.2 | 0.75 ± 0.30 | 0.40 | 0.63 |
| Ga | (−0.01) | 1.6 ± 0.1 | | 0.43 | |
| Ge | (0.02) | 1.9 ± 0.1 | | 0.46 | |

ACKNOWLEDGMENTS

We would like to acknowledge A. Heeres for his experimental assistance and Th. J. van Montfort for executing the numerical Hartree-Fock calculations. This investigation was supported by the Netherlands Foundation for Chemical Research (SON) with financial aid from the Netherlands Organization for the Advancement of Pure Research (ZWO).

[1]E. Antonides, E. C. Janse, and G. A. Sawatzky, Phys. Rev. B 15, 1669 (1977), referred to hereafter as I.
[2]L. I. Yin, I. Adler, M. H. Chen, and B. Crasemann, Phys. Rev. A 7, 897 (1973).
[3]E. D. Roberts, P. Weightman, and C. E. Johnson, J. Phys. C 8, L301 (1975).
[4]J. A. D. Matthew, J. D. Nuttall, and T. E. Gallon, J. Phys. C 9, 883 (1976).
[5]E. Antonides and G. A. Sawatzky, J. Phys. C 9, L547 (1976).
[6]P. Weightman, J. F. McGilp, and C. E. Johnson, J. Phys. C 9, L585 (1976).
[7]E. J. McGuire, Sandia Laboratory Report No. SC-RR-710075, 1971 (unpublished).
[8]L. V. Azâroff, *X-ray Spectroscopy* (McGraw-Hill, New York, 1974), p. 233.